

On the maximum value of the cosmic abundance of oxygen and the oxygen yield

Leonid S. Pilyugin¹, Trinh X.Thuan² and José M. Vílchez³

¹ *Main Astronomical Observatory of National Academy of Sciences of Ukraine, 27 Zabolotnogo str., 03680 Kiev, Ukraine (pilyugin@mao.kiev.ua)*

² *Astronomy Department, University of Virginia, P.O.Box 400325, Charlottesville, VA 22904, USA (ttx@virginia.edu)*

³ *Instituto de Astrofísica de Andalucía, CSIC, Apdo, 3004, 18080 Granada, Spain (jvm@iaa.es)*

Accepted 2006 December 19. Received 2006 December 14; in original form 2006 July 27

ABSTRACT

We search for the maximum oxygen abundance in spiral galaxies. Because this maximum value is expected to occur in the centers of the most luminous galaxies, we have constructed the luminosity – central metallicity diagram for spiral galaxies, based on a large compilation of existing data on oxygen abundances of H II regions in spiral galaxies. We found that this diagram shows a plateau at high luminosities ($-22.3 \lesssim M_B \lesssim -20.3$), with a constant maximum value of the gas-phase oxygen abundance $12+\log(\text{O}/\text{H}) \sim 8.87$. This provides strong evidence that the oxygen abundance in the centers of the most luminous metal-rich galaxies reaches the maximum attainable value of oxygen abundance. Since some fraction of the oxygen (about 0.08 dex) is expected to be locked into dust grains, the maximum value of the true gas+dust oxygen abundance in spiral galaxies is $12+\log(\text{O}/\text{H}) \sim 8.95$. This value is a factor of ~ 2 higher than the recently estimated solar value. Based on the derived maximum oxygen abundance in galaxies, we found the oxygen yield to be about 0.0035, depending on the fraction of oxygen incorporated into dust grains.

Key words: galaxies: abundances – ISM: abundances – H II regions

1 INTRODUCTION

It is well known that there is a large scatter in the heavy element content of galaxies. This is due to the fact that different galaxies evolve chemically at different rates. Galactic winds with different efficiencies can also make a significant contribution to the scatter in metallicity in low-mass dwarf irregular galaxies. The oxygen abundance in the interstellar gas is usually used as a tracer of metallicity in late-type (spiral and irregular) galaxies. A question of great interest in the chemical evolution of galaxies is that of the maximum value of the observed oxygen abundance. Is there such a value? And is this maximum value equal to the maximum attainable value of the oxygen abundance in galaxies?

The latter is defined by the stellar oxygen yield, i.e. the mass of oxygen freshly synthesized and ejected by a generation of stars relative to the mass locked up in low-mass stars and compact remnants. It can be derived within the framework of chemical evolution models of galaxies (Pagel 1997). The closed-box model which neglects mass exchange between a galaxy and its environments gives the maximal upper bound to the metallicity of the gas for a given gas mass fraction (Edmunds 1990). In practice, the procedure is

often inverted, i.e. the measured chemical compositions of galaxies are used to estimate empirically the oxygen yield (e.g. Garnett 2002; Pilyugin et al. 2004). This is so because the theoretical value of the oxygen yield is not well known, due to uncertainties in both the oxygen production by stars of different masses and metallicities and the parameters of the initial mass function of stars, the relative birthrates of stars with different initial masses. Thus the uncertainty in the stellar oxygen yield prevents an accurate determination of the maximum attainable value of the oxygen abundance in galaxies through chemical evolution models of galaxies.

Can we determine that maximum value by observations? Oxygen abundances in the most metal-rich spiral galaxies in the samples of Vila-Costas & Edmunds (1992); Zaritsky et al. (1994); Garnett et al. (1997); van Zee et al. (1998)) have been estimated previously by Pilyugin et al. (2006a). Those authors found the maximum gas-phase oxygen abundance in the central regions of those spiral galaxies to be $12+\log(\text{O}/\text{H}) \sim 8.75$, suggesting that this value may be an upper limit to the oxygen abundances in spiral galaxies.

Here we carry out a search for the maximum oxygen abundance using a considerably larger sample of spi-

ral galaxies. The strategy of our search is based on the two following considerations. First, Lequeux et al. (1979) have found that, for irregular galaxies, the oxygen abundance correlates with the total galaxy mass, in the sense that the higher the total mass, the higher the heavy element content. Since the galaxy mass is a poorly known quantity, the luminosity – metallicity ($L - Z$) relation is often used instead of the mass – metallicity relation. Garnett & Shields (1987) have indeed found that spiral disk abundances correlate well with galaxy luminosities. This luminosity-metallicity correlation has been confirmed in many studies of spiral galaxies (Vila-Costas & Edmunds 1992; Zaritsky et al. 1994; Garnett 2002; Pilyugin et al. 2004; Tremonti et al. 2004). Second, Searle (1971) and Smith (1975) have established many years ago the presence of radial abundance gradients in the disks of spiral galaxies, with the maximum oxygen abundance occurring at their centers. Taken together, these two facts suggest that the observed oxygen abundance should reach its maximal value at the centers of the most luminous galaxies.

In the following, we will be using these notations for the line fluxes : $R_2 = I_{[\text{OII}]\lambda 3727 + \lambda 3729} / I_{H\beta}$, $R_3 = I_{[\text{OIII}]\lambda 4959 + \lambda 5007} / I_{H\beta}$, $R = I_{[\text{OIII}]\lambda 4363} / I_{H\beta}$, $R_{23} = R_2 + R_3$. With these definitions, the excitation parameter P can be expressed as: $P = R_3 / (R_2 + R_3)$. The plan of our study is as follows. In Section 2 we determine the central oxygen abundance for a large sample of nearby spiral galaxies and derive the maximum oxygen abundance. The value of the oxygen yield is estimated in Section 3. We summarize our conclusions in Section 4.

2 THE MAXIMUM VALUE OF THE OXYGEN ABUNDANCE

2.1 Abundance derivation

The $[\text{OIII}]\lambda 4363$ auroral line is not detected in the majority of H II regions in spiral galaxies. For a quarter of a century, different versions of the one-dimensional empirical calibration, first proposed by Pagel et al. (1979), have been used for abundance determination in such H II regions. Pilyugin (2000, 2001a, 2003b) has found that the oxygen abundances so determined have a systematic error, depending on the excitation parameter defined above. Recently, a relationship between the observed auroral and nebular oxygen line fluxes, the ff relation, has been established (Pilyugin 2005; Pilyugin et al. 2006a). The ff relation allows one to estimate the flux in the $[\text{OIII}]\lambda 4363$ auroral line, and hence to apply the T_e method to determine abundances in H II regions where that line is not detected, and where only strong oxygen line intensities are seen. We have also derived a new model-independent $t_2 - t_3$ relation (Pilyugin et al. 2006b)

$$t_2 = 0.72 t_3 + 0.26. \quad (1)$$

We have thus found a way to estimate the electron temperature in both in the O^{++} and in the O^+ zones in high-metallicity H II regions where the $[\text{OIII}]\lambda 4363$ auroral line is not detected. Next, we apply the method described above to derive new oxygen abundances in spiral galaxies. Our aim is to search for a maximum value of the observed oxygen abundance in galaxies.

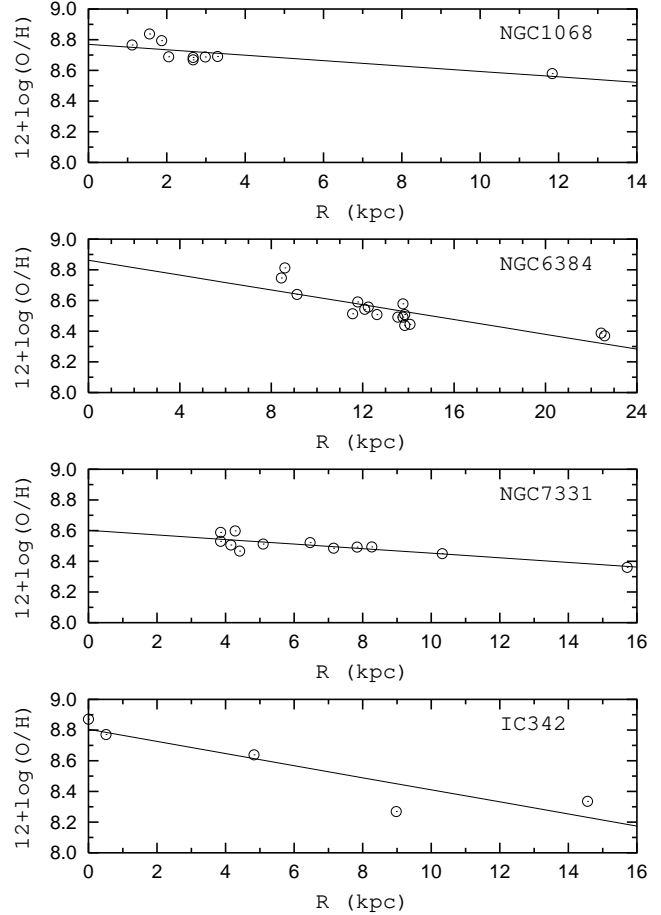


Figure 1. The oxygen abundance as a function of galactocentric distance in the disks of the four most luminous spiral galaxies in our sample: NGC 1068, NGC 6384, NGC 7331 and IC 342. The circles are $(\text{O}/\text{H})_{ff}$ abundances in individual H II regions. The lines are linear least-square best fits to those data points.

2.2 A plateau in the $L - Z$ diagram at high luminosities

We first define our observational sample. We use the compilation by Pilyugin et al. (2004) of a large sample of published spectra of H II regions in nearby spiral galaxies. Recent measurements from Bresolin et al. (2004, 2005); Crockett et al (2006) have been added to that list. Since the maximum value of the observed oxygen abundance is expected to occur at the centers of the most luminous galaxies, we first derive the radial distribution of the oxygen abundance in the disks of the four most luminous spiral galaxies in our sample: NGC 1068 with an absolute blue magnitude $M_B = -22.18$, NGC 6384 with $M_B = -22.22$, NGC 7331 with $M_B = -22.20$, and IC 342 with $M_B = -22.27$. The distances and luminosities of the galaxies are taken from Pilyugin et al. (2004).

Fig. 1 shows the oxygen abundance as a function of galactocentric distance in the disks of the four most luminous spiral galaxies in our sample. The points are $(\text{O}/\text{H})_{ff}$ abundances in individual H II regions. The lines are linear least-square best fits to those points. Inspection of Fig. 1 shows that the central oxygen abundance in the most luminous spiral galaxies can be as large as $12 + \log(\text{O}/\text{H}) \sim 8.87$.

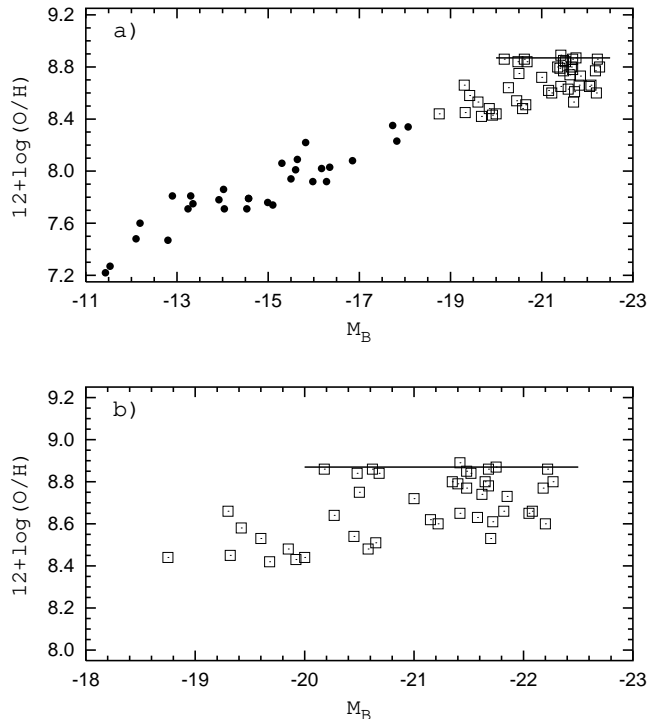


Figure 2. The luminosity – central metallicity diagram. *Top panel.* The open squares show the central $(\text{O}/\text{H})_{\text{ff}}$ abundances in the disks of spiral galaxies plotted against their luminosities. The filled circles denote irregular galaxies from Pilyugin et al. (2004). *Bottom panel.* A blow-up of the high-luminosity part of the L – Z diagram in the top panel.

Are those galaxies indeed the most oxygen-rich ones as expected from the L – Z correlation? To clarify this point, we next derive the central oxygen abundances of all the spiral galaxies in our sample and examine their dependence on galaxian luminosity.

The top panel of Fig. 2 shows the familiar L – Z relation, where Z denotes here the central oxygen abundance. The squares show the central $(\text{O}/\text{H})_{\text{ff}}$ abundances of the spiral galaxies in our sample. For the majority of galaxies, all H II regions with available oxygen emission line measurements have been used in the abundance gradient analysis. For a few galaxies however, some H II regions have been omitted for the following reason. The $R_{23} - \text{O}/\text{H}$ relation is double-valued, with two distinct parts usually known as the “lower” and “upper” branches. The ff relation is valid only for H II regions which are located in the upper branch, with $12+\log(\text{O}/\text{H})$ higher than ~ 8.25 . Thus, one has to know *a priori* on which of the two branches the H II region lies. Given that disks of spiral galaxies show radial oxygen abundance gradients, in the sense that the oxygen abundance is higher in the central part of the disk and decreases with galactocentric distance, we first consider H II regions in the central part of disks and move outward until the radius R^* , where the oxygen abundance decreases to $12+\log(\text{O}/\text{H}) \sim 8.25$. The exact value of R^* is somewhat uncertain due to the scatter in the oxygen abundance values at any fixed radius. It should be emphasized that a misuse of ff relation in the determination of the oxygen abundance in low-metallicity H II regions beyond R^* may produce an artificial change of

slope at R^* in the abundance gradients (Pilyugin 2003a). Therefore, H II regions with galactocentric distances larger than R^* , i.e. those with $12+\log(\text{O}/\text{H})$ less than 8.25 were rejected.

The filled circles in Fig. 2 show irregular galaxies from Pilyugin (2001b); Pilyugin et al. (2004). Our L – Z diagram for irregular galaxies is in good agreement with the ones derived by other authors (Richer & McCall 1995; Lee et al. 2003). Examination of Fig. 2 shows that the central oxygen abundances in galaxies with $M_B \sim -20.25$ are in the same range as those of galaxies with $M_B \sim -22.25$, i.e. the central oxygen abundances in luminous galaxies with $M_B < -20.25$ do not show an appreciable correlation with galaxy luminosity. This flattening of the L – Z relation can be seen more clearly in the bottom panel of Fig. 2 which shows a blow-up of the high-luminosity end of the relation. The presence of an upper envelope in the L – Z relation at $12+\log(\text{O}/\text{H}) \sim 8.87$, is clearly seen. The flattening of the L – Z relation at high luminosities has been noted before by Pilyugin et al. (2004); Tremonti et al. (2004).

What is the meaning of such a plateau? There are two known reasons for the existence of the L – Z relation. First, it can be caused by a dependence of the efficiency of galactic winds to get rid of metals on the galaxy’s luminosity: more luminous and massive galaxies are less efficient in losing heavy elements by galactic winds. In this case, the L – Z relation represents the ability of a given galaxy to retain the products of its own chemical evolution rather than its ability to produce metals (Larson 1974). It is believed that the galactic winds do not play a significant role in the chemical evolution of the largest spiral galaxies (e.g. Garnett 2002; Pilyugin et al. 2004; Tremonti et al. 2004). The second reason that has been invoked to explain the L – Z relation, which we adopt, is that the astration level increases and the gas mass fraction decreases as the luminosity of a galaxy increases (McGaugh & de Blok 1997). The existence of a plateau at high luminosities in the L – Z relation thus implies that, on average, the central parts of large luminous spiral galaxies have similar astration levels.

Another prominent feature of the L – Z relation is the rather large scatter in oxygen abundances at a given luminosity, $\Delta\log(\text{O}/\text{H}) \sim 0.25$. Part of this scatter may be due to uncertainties in the oxygen abundances. But another part is likely to be real. This scatter may be explained by fluctuations of the gas mass fraction μ among galaxies of a given luminosity. The simple model of chemical evolution of galaxies predicts that a decrease of μ by 0.1 results in an increase of the oxygen abundance by ~ 0.13 dex, in the range of μ from ~ 0.50 to ~ 0.05 . Then, a scatter $\Delta\log(\text{O}/\text{H}) \sim 0.25$ may be explained by fluctuations of the gas mass fraction as large as $\Delta\mu \sim 0.2$ among galaxies of a given luminosity. The global gas mass fractions in the sample spiral galaxies have been estimated to be low, $\mu < 0.25$ (Garnett 2002; Pilyugin et al. 2004). This suggests that the gas in the centers of the most metal-rich galaxies has been almost completely converted into stars. Consequently, the observed oxygen abundance in the centers of those galaxies represents the maximum attainable value of the oxygen abundance. This provides a natural explanation for the constant maximum value of the observed central oxygen abundance in the most oxygen-rich galaxies (Fig. 2).

The maximum value of the gas-phase oxygen abun-

dance in H II regions of spiral galaxies is thus $12+\log(\text{O}/\text{H}) \sim 8.87$. Some fraction of the oxygen is locked into dust grains (Meyer et al. 1998; Esteban et al. 1998). According to Esteban et al. (1998), the fraction of the dust-phase oxygen abundance in the Orion nebula is about 0.08 dex (but see Simón-Díaz et al. (2006)). Then, the maximum value of the gas+dust oxygen abundance in H II regions of spiral galaxies is $12+\log(\text{O}/\text{H}) \sim 8.95$.

2.3 Discussion

The oxygen abundances we have derived here for luminous spiral galaxies are significantly lower than those obtained previously by a number of previous investigators (Garnett 2002; Tremonti et al. 2004; Melbourne & Salzer 2002; Lamareille et al. 2004). This is not surprising. The abundances in the papers quoted above have been derived using different versions of the early calibration. It has been argued (Pilyugin 2001a; Pilyugin et al. 2004) that the oxygen abundances so determined are significantly overestimated at the high-metallicity end. Indeed, Tremonti et al. (2004) have themselves noted that their oxygen abundances may have been overestimated by as much as a factor of two. On the other hand, the oxygen abundances obtained here are not based on any calibration since they are derived via the T_e method coupled with the ff relation. The ff relation is purely empirical in the sense that it relates directly measured quantities, without any other assumption.

The central oxygen abundances of two luminous spiral galaxies, M 101 ($M_B = -21.65$) and M 51 ($M_B = -21.48$), have recently been determined from measurements of $(\text{O}/\text{H})_{T_e}$ abundances in a number of H II regions. They have been found to be respectively $12+\log(\text{O}/\text{H})_{T_e} = 8.76$ (Kennicutt et al. 2003), and $12+\log(\text{O}/\text{H})_{T_e} = 8.72$ (Bresolin et al. 2004). Those data are in agreement with our L – Z relation, but are in severe conflict with relations based on O/H abundances derived with the one-dimensional empirical calibrations.

Comparison with H II region photoionization models has led some authors (e.g. Stasińska 2005) to question the applicability of the classic T_e method to the high-metallicity regime. We have suggested (Pilyugin 2003b) using the interstellar oxygen abundance in the solar vicinity, derived with very high precision from high-resolution observations of the weak interstellar OI λ 1356 absorption line towards the stars, as a "Rosetta stone" to check the reliability of the oxygen abundances derived in H II regions with the T_e method. The agreement between the value of the oxygen abundance at the solar galactocentric distance derived from the T_e method and that derived from the OI λ 1356 interstellar absorption line towards the stars provides strong support for the applicability of the classic T_e method to solar-metallicity objects. We have also examined previously the reliability of oxygen abundances derived in high-metallicity H II regions with the T_e method by analyzing the radial distributions of oxygen abundances in the disks of spiral galaxies (Pilyugin et al. 2006a). According to Stasińska (2005), the derived $(\text{O}/\text{H})_{T_e}$ value is very close to the real one as long as the metallicity is low. Discrepancies appear for oxygen abundances $12+\log(\text{O}/\text{H}) \sim 8.6 - 8.7$, and may become very large as metallicity increases (Fig. 1a in Stasińska 2005). The derived $(\text{O}/\text{H})_{T_e}$ values are smaller than the real ones, some-

times by enormous factors. If this is the case, then the radial distribution of $(\text{O}/\text{H})_{T_e}$ abundances should show a bow-shaped curve with a maximum value of $12+\log(\text{O}/\text{H}) \sim 8.7$ at some galactocentric distance. However, the derived radial distributions of $(\text{O}/\text{H})_{T_e}$ abundances in the disks of spiral galaxies do not show such an appreciable curvature, and the $(\text{O}/\text{H})_{T_e}$ abundances increase more or less monotonically with decreasing galactocentric distance (Pilyugin et al. 2006a). Thus, while our results do not rule out the possible existence of the Stasińska's effect, they suggest that the great majority of H II regions in galaxies are in a metallicity range where this effect is not important. Another factor that may affect our abundance determinations is temperature fluctuations inside H II regions (Peimbert 1967). If they are important, our abundances would be underestimated.

The abundances derived here thus depend on the ability of the classic T_e method to give correct abundances in the high-metallicity regime. They will be subject to revision if, when metal-rich H II regions are better understood, it is shown that the T_e method, because of temperature fluctuations, strong electron temperature gradients inside H II regions, or any other reason, results in incorrect abundances at high metallicities.

The Sun is one of the widely used reference objects in astrophysics. Standard practice is to express the element content in a cosmic object via the corresponding value for the Sun, i.e. the composition of the Sun is used as standard unit. For many years, the recommended solar oxygen abundance was $12+\log(\text{O}/\text{H})_{\odot} \approx 8.9$. This high abundance was obtained from a one-dimensional hydrostatic model of the solar atmosphere. Recently the solar oxygen abundance has been significantly reduced as a result of a time-dependent, three-dimensional hydrodynamical model of the solar atmosphere. Taking the average of recent determinations ($12+\log(\text{O}/\text{H})_{\odot} = 8.70$ in Allende Prieto et al. (2004), 8.66 in Asplund et al. (2004), 8.59 in Meléndez (2004)), the solar abundance is now $12+\log(\text{O}/\text{H})_{\odot} = 8.65$. Thus, the maximum value of the gas+dust oxygen abundance of H II regions in spiral galaxies is higher by a factor of ~ 2 than the solar value.

3 THE OXYGEN YIELD

3.1 Basic considerations

The simple model of chemical evolution of galaxies predicts that the oxygen abundance of the interstellar matter of a galaxy is related to the gas mass fraction μ and the oxygen yield Y_{O} by the following formula

$$Y_{\text{O}} = \frac{Z_{\text{O}}}{\ln(\frac{1}{\mu})}. \quad (2)$$

In a real situation, the oxygen abundance is also affected by the mass exchange between a galaxy and its environment. This mass exchange can alter the above relation and mimic a variation in the oxygen yield. In that case, the simple chemical evolution model is used to estimate the "effective" oxygen yield Y_{eff} (Edmunds 1990; Vila-Costas & Edmunds 1992)

As noted above, it is believed that galactic winds do not play a significant role in the chemical evolution of the

largest spiral galaxies. For these, is the oxygen yield derived by using Eq. (2) close to the true oxygen yield? This may not be the case for two reasons. First, the simple model is based on the instantaneous recycling approximation. Oxygen is produced and ejected into the interstellar medium by massive stars with lifetimes much shorter than the evolution time of spiral galaxies. From this point of view, the instantaneous recycling approximation is justified. However, the value of Y_{O} depends not only on the amount of oxygen but also on the total mass of matter ejected in the interstellar medium (see below). In other words, the instantaneous recycling approximation assumes that the next generation of star is formed when all stars from previous generations have finished their evolution. This never occurs in a real galaxy. As a consequence, the simple model predicts slightly higher oxygen abundances than numerical models for the chemical evolution of galaxies with realistic star formation histories (Pilyugin 1994). Fortunately, this difference is small and can be neglected in the case of oxygen.

Furthermore, it is well known that the simple model predicts many more low-metallicity stars than are observed in the solar neighbourhood, the so called ‘‘G-dwarf’’ paradox. Various versions of the infall model, in which an infall of gas onto the disk takes place for a long time, have been proposed to account for the observed metallicity distribution in the solar neighborhood. (Tosi 1988a,b; Pilyugin & Edmunds 1996a,b; Chiappini et al. 2001, among many others). An infall model has also been applied to other spiral galaxies (Pagel 1997, and references therein). It is thus generally accepted that gas infall plays an important role in the chemical evolution of disks of spiral galaxies. Therefore, the application of the simple model to large spiral galaxies to estimate the true oxygen yields may appear unjustified. It is expected that the rate of gas infall onto the disk decreases exponentially with time (e.g. Pilyugin & Edmunds 1996a,b). It has been shown (Pilyugin & Ferrini 1998) that the present-day location of a system in the $\mu - \text{O}/\text{H}$ diagram is governed by its evolution in the recent past, but is independent of its evolution on long timescales. Therefore, the fact that the present-day location of spiral galaxies is near the one predicted by the simple model is not in conflict with a picture in which an infall of gas onto the disk takes place during a long time (the latter is necessary to satisfy the observed abundance distribution function and the age – metallicity relation in the solar neighbourhood) since these observational data reflect the evolution of the system in the distant past. Therefore, one can expect that the application of the simple model to large spiral galaxies, Eq. (2), provides a more or less reasonable estimate of the true oxygen yield Y_{O} . Certainly, to find an accurate value of the true oxygen yield Y_{O} , an appropriate models of chemical evolution of galaxies should be computed.

3.2 An empirical estimate of the oxygen yield

From Eq. (2), it is clear that an accurate determination of the oxygen yield depends on accurate oxygen abundance and gas mass fraction measurements. Our derived $(\text{O}/\text{H})_{\text{ff}}$ abundances are more accurate than the $(\text{O}/\text{H})_{\text{R}23}$ abundances used in previous studies. However, a precise estimate of the gas mass fraction is not a trivial task, and this for several reasons. On the one hand, the mass of the stellar component

of a galaxy is usually estimated by converting the measured luminosity to mass via an adopted mass-to-luminosity ratio. The latter is strongly model-dependent, therefore it is difficult to get a reliable estimate of it for individual galaxies. It is widely accepted that the converting factor from the near-infrared luminosity is a robust quantity for deriving the stellar mass of a galaxy. This quantity shows a low dependence on the star formation history but depends strongly on the initial mass function (for example, on the adopted lower stellar mass limit). On the other hand, the mass of molecular hydrogen can only be estimated by indirect methods. The commonly accepted method is the use of the CO line flux and a conversion factor X between the flux in the CO line and the amount of molecular hydrogen. The conversion factor $X = \text{N}(\text{H}_2)/\text{I}(\text{CO})$ depends strongly on the physical properties of the interstellar medium which are known to vary from galaxy to galaxy. The best-estimated values of X for a sample of well-studied nearby galaxies span the range from 0.6 to $10 \times 10^{20} \text{ mol cm}^{-2} (\text{K km s}^{-1})^{-1}$ (Boselli et al. 2002). Thus, the value of the oxygen yield derived from Eq. (2) can be strongly affected by the uncertainty in the gas mass fraction determination.

The use of the maximum value of the oxygen abundance derived here allows us to overcome the above problem in the following way. We compare the derived maximum value of the oxygen abundance in galaxies with oxygen abundances predicted by the simple models with different oxygen yields for $\mu=0$. Fig. 3 shows the oxygen abundance as a function of the gas mass fraction predicted by the simple model with $Y_{\text{O}}=0.0030$ (solid line) and with $Y_{\text{O}}=0.0035$ (dashed line). Since the oxygen abundances are expressed in units of number of oxygen atoms relative to hydrogen, while Z_{O} in Eq. (2) have units of mass fraction, we adopt the following conversion equation for oxygen (Garnett 2002)

$$Z_{\text{O}} = 12 \frac{O}{H}. \quad (3)$$

The simple model breaks down as the gas mass fraction approaches zero because the term $\ln(1/\mu)$ blows up. Therefore the oxygen abundance predicted by the simple model at $\mu=0$ should be estimated by extrapolation of the model predictions to $\mu=0$. The extrapolations of the simple models for two values of the oxygen yield are shown in Fig. 3 by the dotted lines. The fact that the central oxygen abundances in galaxies are derived here, not as oxygen abundances of H II regions in the very central parts of galaxies, but also as extrapolations of linear fits, justifies the above method.

The maximum value of the observed gas-phase oxygen abundance in H II regions of spiral galaxies is shown by the open square in Fig. 3. The maximum value of the gas+dust oxygen abundance is shown by the open circle. Examination of Fig. 3 shows that the maximum value of the observed gas-phase oxygen abundance in H II regions of spiral galaxies corresponds to the simple model with $Y_{\text{O}} \sim 0.0030$, and the maximum value of the gas+dust oxygen abundance in spiral galaxies corresponds to the simple model with $Y_{\text{O}} \sim 0.0035$.

Thus, we can conclude that the value of the oxygen yield is about 0.0035, depending on the fraction of oxygen incorporated into dust grains. The value of the oxygen yield derived here from the gas-phase oxygen abundance ($Y_{\text{O}} \approx 0.0030$) is close to that obtained recently for spiral galaxies by Pilyugin et al. (2004) ($Y_{\text{O}} \approx 0.0027$) and

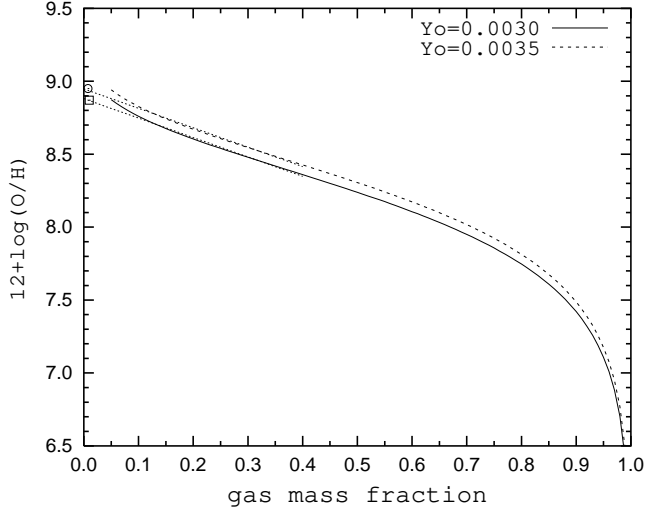


Figure 3. The oxygen abundance as a function of the gas mass fraction predicted by the simple models of chemical evolution of galaxies, with an oxygen yield $Y_{\text{O}}=0.0030$ (solid line) and with $Y_{\text{O}}=0.0035$ (dashed line). The extrapolations to $\mu=0$ for these models are shown by the dotted lines. The open square is the maximum value of the observed gas-phase oxygen abundance in H II regions of spiral galaxies. The open circle is the maximum value of the gas+dust oxygen abundance.

by Bresolin et al. (2004) ($Y_{\text{O}} \approx 0.0032$), but is significantly lower than the oxygen yield obtained by Garnett (2002) ($Y_{\text{O}} \approx 0.010$).

3.3 The stellar oxygen yield

Can the derived value of Y_{O} be reproduced by the existing stellar evolution models? The similarity between the present oxygen abundances in the interstellar matter in the solar vicinity and that in the Sun which was set up some 4.5 Gyr ago, suggests that spiral galaxies have had a high oxygen abundance during most of their evolution. We therefore use estimates of the yields in the high-metallicity regime. We have compiled the yields at solar metallicity from several sources (Maeder 1992; Woosley & Weaver 1995; Langer & Henkel 1995; Nomoto et al. 1997; Portinari et al. 1998; Meynet & Maeder 2002; Hirschi et al. 2005; Kobayashi et al. 2006). Following Timmes et al. (1995), we have used models A from Woosley & Weaver (1995) for stars in the 11 - 25 M_{\odot} mass range, and models B for masses equal to 30, 35, and 40 M_{\odot} . The yields computed by Meynet & Maeder (2002) for the metallicity $Z = 0.020$ are given in Chiappini et al. (2003a). The mass M_{O} of freshly produced oxygen ejected by a star in the interstellar medium, calculated by different authors, is shown as a function of the initial stellar mass in the top panel of Fig. 4. That figure shows that there exists significant differences between the various predictions of M_{O} at a given initial stellar mass. The differences are especially large for stellar masses larger than $\sim 25 M_{\odot}$. They are caused by differences in the input physics (stellar wind, mixing, etc) used by the various authors. Close examination of the top panel of Fig. 4 reveals that there are two main groups of points: a group of high M_{O} values from Maeder (1992); Woosley & Weaver (1995); Nomoto et al.

(1997); Kobayashi et al. (2006), based on stellar models with small mass loss rates from stellar winds; and a group of low M_{O} values from Maeder (1992); Langer & Henkel (1995); Portinari et al. (1998), based on stellar models with large mass loss rates from stellar winds. We will consider both the high and low values of M_{O} . They can be considered as delimiting the range of oxygen production by stars.

It worth noting that the oxygen production is computed for single stars. A large fraction of stars are members of binary systems and evolve with mass exchange between components. Therefore one may expect that the stellar evolution models with strong stellar winds give values of the oxygen yield that are closer to the true value.

The cumulative mass Q_{O} of freshly manufactured oxygen ejected by a single stellar population at time τ after its formation is calculated as the sum of contributions from each star down to a stellar mass M_{S}^* , corresponding to a lifetime τ . It is given by the following expression

$$Q_{\text{O}}(M_{\text{S}}^*, M_{\text{U}}) = \sum_{M_{\text{S}}^*}^{M_{\text{U}}} M_{\text{O}} \varphi \Delta M_{\text{S}} \quad (4)$$

where $\varphi \Delta M_{\text{S}}$ is the number of stars within the mass interval ΔM_{S} as determined from the initial mass function φ , and M_{O} is the ejected mass of freshly manufactured oxygen from a star with mass M_{S} . Since stars with masses lower than 10 M_{\odot} do not manufacture an appreciable amount of oxygen, the lower mass limit M_{S}^* in Eq. (4) has been set to 10 M_{\odot} . Difficulties arise in the computation of Q_{O} because of the limited number of stellar masses for which models exist. The gaps between the masses for which models have been calculated produce artificial jumps in the resulting $Q_{\text{O}}(M_{\text{U}}, M_{\text{S}}^*)$ (Pilyugin 1992, 1994). To overcome these difficulties, we have adopted the following approach. The dependence of the ejected mass of freshly manufactured oxygen M_{O} on stellar mass M_{S} is approximated by a polynomial of degree 3. We have adopted the approximation

$$\log M_{\text{O}} = -23.29 + 38.84 \log M_{\text{S}} - 21.02 (\log M_{\text{S}})^2 + 3.84 (\log M_{\text{S}})^3 \quad (5)$$

for the case of models with no or low stellar wind mass loss rates. This relation is shown by the solid line in the top panel of Fig. 4. As for the case of models with high stellar wind mass loss rates, we adopt the approximation

$$\log M_{\text{O}} = -24.04 + 41.69 \log M_{\text{S}} - 23.66 (\log M_{\text{S}})^2 + 4.46 (\log M_{\text{S}})^3 \quad (6)$$

This relation is shown by the dashed line in the top panel of Fig. 4. Model points with large deviations were not used in the derivation of these two approximations.

The dependence of the mass M_{ret} of the matter returned by a star to the interstellar medium on the initial mass of the star is shown in the bottom panel of Fig. 4. Inspection of the figure shows that there is agreement between the M_{ret} values from different authors, so that all the data can be approximated by the following expression

$$\log M_{\text{ret}} = -0.344 + 1.666 \log M_{\text{S}} - 0.500 (\log M_{\text{S}})^2 + 0.126 (\log M_{\text{S}})^3 \quad (7)$$

The cumulative mass Q_{ret} returned by a single stellar pop-

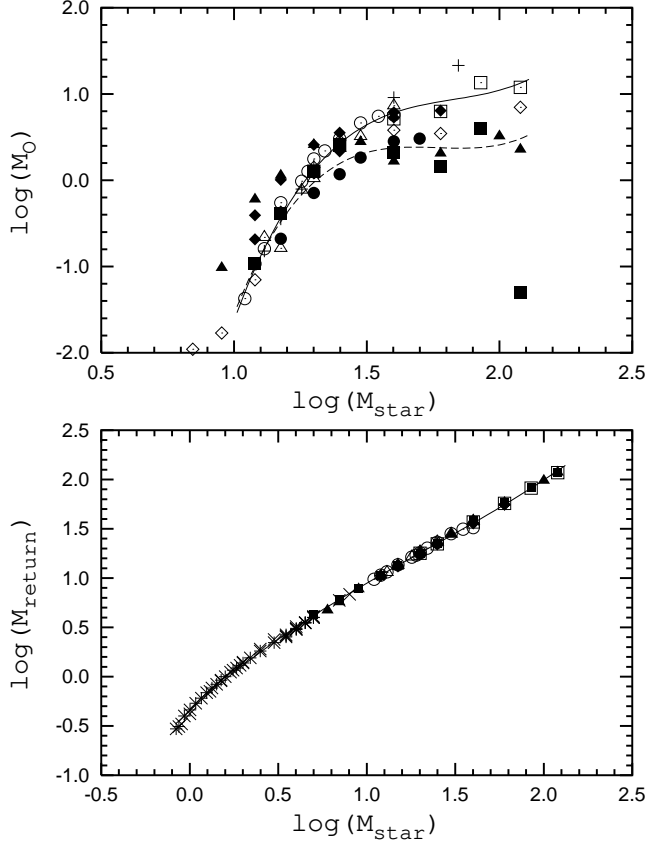


Figure 4. *Top panel.* The mass of freshly manufactured oxygen ejected by a star in the interstellar medium as a function of the initial mass of the star. The results from Maeder (1992) for models with low stellar wind mass loss rates are shown by open squares, and that for models with high stellar wind mass loss rates are shown by filled squares. Results from other investigators have also been plotted: Langer & Henkel (1995) (filled circles), Nomoto et al. (1997) (plus signs), Portinari et al. (1998) (filled triangles), Meynet & Maeder (2002) (open rhombus), Hirschi et al. (2005) (filled rhombus), and Kobayashi et al. (2006) (open triangles). The solid line is a fit to the model results of Maeder (1992) (models with low stellar wind mass loss rates), Woosley & Weaver (1995), Nomoto et al. (1997), and Kobayashi et al. (2006). The dashed line is a fit to the model results of Maeder (1992) (models with high stellar wind mass loss rates), Langer & Henkel (1995) and Portinari et al. (1998). *Bottom panel.* The mass returned by a star to the interstellar medium as a function of the initial mass of the star. The data for low- and intermediate-mass stars from van den Hoek & Groenewegen (1997) are shown by crosses, those from Marigo (2001) by open circles. The sources for the models and the symbols for massive stars are the same as in the top panel. The solid line is a fit to all the data.

ulation is given by the following expression

$$Q_{\text{ret}}(M_S^*, M_U) = \sum_{M_S^*}^{M_U} M_{\text{ret}} \varphi \Delta M_S. \quad (8)$$

To compute Q_O and Q_{ret} , we have to precise the initial mass function (IMF). We first consider the Salpeter (1955) IMF

$$\phi(M_S) = c M_S^{-2.35}. \quad (9)$$

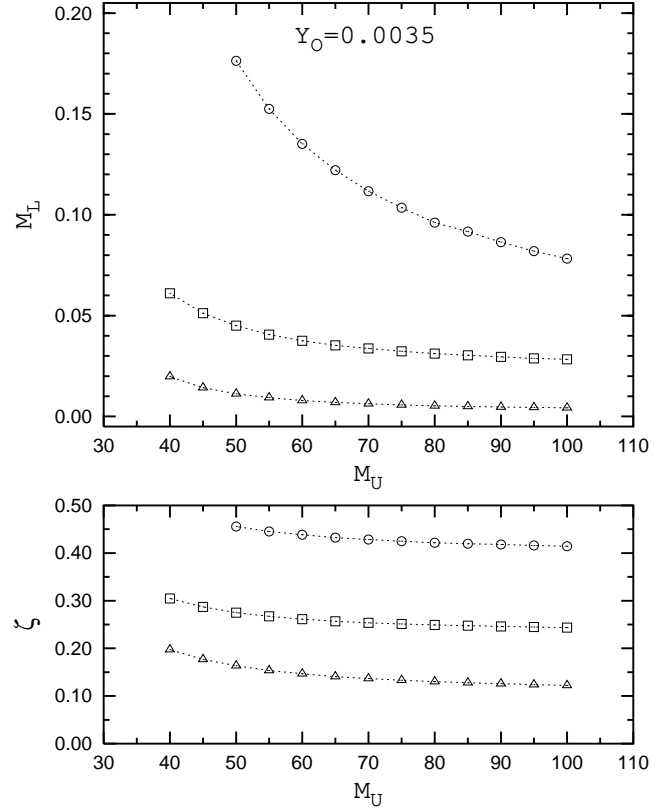


Figure 5. *Top panel.* The lower mass limit M_L of the Initial Mass Function (IMF) calculated so that, for a given upper mass limit M_U , the oxygen yield Y_O is equal to 0.0035. The circles correspond to Kroupa’s IMF and oxygen yields given by stellar models with high stellar wind mass loss rates. The squares correspond to a Salpeter IMF and oxygen yields given by stellar models with high stellar wind mass loss rates. The triangles correspond to a Salpeter IMF and oxygen yields given by stellar models with low stellar wind mass loss rates. Masses are in units of solar masses. *Bottom panel.* The fraction ζ of the total stellar mass in stars with masses above $1M_\odot$ for the three combinations of IMF parameters and oxygen yields in the top panel.

The coefficient c is defined by normalizing the IMF over the whole mass interval

$$\int_{M_L}^{M_U} M_S \phi(M_S) dM_S = 1 \quad (10)$$

where M_L and M_U are the lower and upper mass limits. These mass limits are not known and are in fact free parameters. For example, Romano et al. (2005) adopt $M_U = 100M_\odot$ while Kobayashi et al. (2006) choose $M_U = 50M_\odot$. Sometimes, the fraction ζ of the total stellar mass locked up in stars with masses above $1M_\odot$ is fixed, instead of M_L . Portinari et al. (1998) have found that a “good range” for ζ is between 0.3 and 0.4.

We next check whether there exist values of M_L and M_U so that $Y_O^{\text{mod}} = Y_O$, where the model oxygen yield Y_O^{mod} is, by definition, the ratio of the mass of newly manufactured oxygen ejected by a single stellar population to the mass locked up in long-lived stars or remnants of that single stellar population

$$Y_{\text{O}}^{\text{mod}} = \frac{Q_{\text{O}}(M^*)}{1 - Q_{\text{ret}}(M^*)}. \quad (11)$$

Since stars with masses less than $0.95 M_{\odot}$ have lifetimes longer than the Hubble time (Schaller et al. 1992), we set $M^* = 0.95 M_{\odot}$ in Eqs. (8,11). Then, by fixing $Y_{\text{O}}^{\text{mod}} = 0.0035$ and M_{U} , we can find M_{L} . The resulting dependence of M_{L} on M_{U} is shown in the upper panel of Fig.5. The triangles correspond to oxygen productions of stellar models with low stellar wind mass loss rates (Eq. (5)), while the squares correspond to oxygen productions of stellar models with high stellar wind mass loss rates (Eq. (6)). The lower panel of Fig.5 shows by the same symbols the fraction ζ of the total stellar mass in stars with masses above $1M_{\odot}$, for the same combinations of IMF parameters and oxygen productions as in the upper panel.

A number of multi-component power-law stellar IMFs have been proposed as well. The one from Kroupa et al. (1993) is often used in the construction of chemical evolution models of galaxies. Romano et al. (2005) have found that the Kroupa IMF fits better several observed properties of the solar vicinity as compared to the Salpeter IMF. The three-component power-law IMF of Kroupa et al. (1993) can be parameterized as follows

$$\phi(M_{\text{S}}) = \begin{cases} c_1 M_{\text{S}}^{-1.3} & \text{for } M_{\text{S}} < 0.5 M_{\odot} \\ c_2 M_{\text{S}}^{-2.2} & \text{for } 0.5 M_{\odot} < M_{\text{S}} < 1 M_{\odot} \\ c_2 M_{\text{S}}^{-2.7} & \text{for } M_{\text{S}} > 1 M_{\odot} \end{cases} \quad (12)$$

The coefficients c_1 and c_2 are defined by normalizing the IMF over the whole mass interval (Eq. (10)), and by the condition $c_1 M_{\text{S}}^{-1.3} = c_2 M_{\text{S}}^{-2.2}$ for $M_{\text{S}} = 0.5M_{\odot}$.

The dependence of M_{L} on M_{U} for the Kroupa IMF and for oxygen productions from models with high stellar wind mass loss rates (Eq. (6)) is shown by circles in the top panel of Fig.5. The bottom panel shows also by circles the fraction ζ of the total stellar mass in stars with masses above $1M_{\odot}$, for the same IMF parameters and oxygen productions as in the top panel. The value $Y_{\text{O}} = 0.0035$ cannot be reproduced with a Kroupa IMF and oxygen productions from models with low stellar wind mass loss rates.

In summary, we have found that in the case of a Salpeter IMF, the observed yield, $Y_{\text{O}} = 0.0035$, can be satisfactorily reproduced by existing stellar evolution models with both low and high stellar wind mass loss rates. However, in the case of a Kroupa IMF, the observed yield can only be reproduced by stellar evolution models with high stellar wind mass loss rates. If the Kroupa IMF is more realistic than the Salpeter IMF, then our results suggest that stellar evolution models with low stellar wind mass loss rates predict too large oxygen yields. In the case of stellar models with high stellar wind mass loss rates, we obtain $\zeta \sim 0.25$ for a Salpeter IMF and $\zeta \sim 0.40$ for a Kroupa IMF. These values are close to the ‘‘good range’’, $0.3 < \zeta < 0.4$, found by Portinari et al. (1998).

The above conclusion is at odds with the finding of Chiappini et al. (2003b) that the oxygen yields in massive stars computed by Woosley & Weaver (1995) without taking into account mass loss reproduce well abundance observations in the spiral galaxy M 101. The origin of the divergences in Chiappini et al. (2003b) conclusions and ours probably comes from the fact that those authors used an early higher value of the central oxygen abundance of M 101, $12+\log(\text{O}/\text{H}) \sim 9.2$, while recent measurements of $(\text{O}/\text{H})_{\text{T}_e}$

abundances in a number of H II regions in M 101 have given a central oxygen abundance $12+\log(\text{O}/\text{H})_{\text{T}_e} = 8.76$ (Kennicutt et al. 2003).

4 CONCLUSIONS

We search here for the maximum oxygen abundance in spiral galaxies. It is expected that this maximum value occurs at the centers of the most luminous galaxies. The luminosity – central metallicity diagram for spiral galaxies is constructed. The central oxygen abundance in a galaxy is derived from a linear least-square best fit to the abundances in individual H II regions at various galactocentric distances. The oxygen abundance in an H II region is derived using the T_e method, with the flux in the [OIII] λ 4363 auroral line determined from the ff relation when not available from observations. The electron temperature t_2 is estimated from a newly derived $t_2 - t_3$ relation (Pilyugin et al. 2006b).

We found that there exists a plateau in the luminosity – central metallicity diagram at high luminosities ($-22.3 \lesssim M_B \lesssim -20.3$). This provides strong evidence that the oxygen abundance in the centers of the most metal-rich luminous spiral galaxies reaches the maximum attainable value of oxygen abundance. The maximum value of the gas-phase oxygen abundance in H II regions of spiral galaxies is $12+\log(\text{O}/\text{H}) \sim 8.87$. Because some fraction of the oxygen (about 0.08 dex) is expected to be locked into dust grains, the maximum value of the true gas+dust oxygen abundance in H II regions of spiral galaxies is $12+\log(\text{O}/\text{H}) \sim 8.95$. This value is a factor of ~ 2 higher than the recently estimated solar value.

Based on our derived maximum value of the oxygen abundance in spiral galaxies, we have estimated the oxygen yield. We have found that the oxygen yield is around 0.0035, depending on the fraction of oxygen incorporated into dust grains.

Acknowledgments

We thank the referee, Grazyna Stasińska, for helpful comments. This research was made possible in part by Award No. UP1-2551-KV-03 of the US Civilian Research & Development Foundation for the Independent States of the Former Soviet Union (CRDF). T.X.T. has been partially supported by NSF grant AST-02-05785. T.X.T. thanks the hospitality of the Institut d’Astrophysique in Paris and of the Service d’Astrophysique at Saclay during his sabbatical leave. He is grateful for a Sesquicentennial Fellowship from the University of Virginia.

REFERENCES

- Allende Prieto C., Asplund M., Fabiani Bendicho P., 2004, *A&A*, 423, 1109
- Asplund M., Grevesse N., Sauval A.J., Allende Prieto C., Kiselman D., 2004, *A&A*, 417, 751
- Boselli A., Lequeux J., Gavazzi G., 2002, *A&A*, 384, 33
- Bresolin F., Garnett, D.R., Kennicutt R.C., 2004, *ApJ*, 615, 228

- Bresolin F., Schaerer D., González Delgado R.M., Stasińska G., 2005, *A&A*, 441, 981
- Chiappini C., Matteucci F., Romano D., 2001, *ApJ*, 554, 1044
- Chiappini C., Matteucci F., Meynet G., 2003a, *A&A*, 410, 275
- Chiappini C., Romano D., Matteucci F., 2003b, *MNRAS*, 339, 63
- Crockett N.R., Garnett D.R., Massey P., Jacoby G., 2006, *ApJ*, 637, 741
- Edmunds M.G., 1990, *MNRAS*, 246, 678
- Esteban C., Peimbert M., Torres-Peimbert S., Escalante V., 1998, *MNRAS*, 295, 401
- Hirschi R., Meynet G., Maeder A., 2005, *A&A*, 433, 1013
- Garnett D.R., 2002, *ApJ*, 581, 1019
- Garnett D.R., Shields G.A., 1987, *ApJ*, 317, 82
- Garnett D.R., Shields G.A., Skillman E.D., Sagan S.P., Dufour R.J., 1997, *ApJ*, 489, 63
- Kennicutt R.C., Bresolin F., Garnett D.R., 2003, *ApJ*, 591, 801
- Kobayashi C., Umeda H., Nomoto K., Tominaga N., Ohkubo T., 2005, *ApJ*, in press (astro-ph/0608688)
- Kroupa P., Tout C.A., Gilmore G., 1993, *MNRAS*, 262, 545
- Lamareille F., Mouchine M., Contini T., Lewis I., Maddox S., 2004, *MNRAS*, 350, 396
- Langer N., Henkel C., 1995, *Sp. Sci. Rev.*, 74, 343
- Larson R.B., 1974, *MNRAS*, 169, 229
- Lee H., McCall M.L., Kingsburgh R.L., Ross R., Stevenson C.C., 2003, *AJ*, 125, 146
- Lequeux J., Peimbert M., Rayo J.F., Serrano A., Torres-Peimbert S., 1979, *A&A*, 80, 155
- Maeder A., 1992, *A&A*, 264, 105
- Marigo P., 2001, *A&A*, 370, 194
- McGaugh S.S., de Blok W.J.G., 1997, *ApJ*, 481, 689
- Melbourne J., Salzer J.J., 2002, *AJ*, 123, 2302
- Meléndez J., 2004, *ApJ*, 615, 1042
- Meyer D.M., Jura M., Cardelli, J.A., 1998, *ApJ*, 493, 222
- Meynet G., Maeder A., 2002, *A&A*, 390, 561
- Nomoto K., Hashimoto M., Tsujimoto T., Thielemann F.-K., Kishimoto N., Kubo Y., Nakasato, N., 1997, *Nucl. Phys. A.*, 616, 79
- Pagal B.E.J., 1997, *Nucleosynthesis and Chemical Evolution of Galaxies*, (Cambridge University Press, Cambridge, 1997)
- Pagal B.E.J., Edmunds M.G., Blackwell D.E., Chun M.S., Smith, G., 1979, *MNRAS*, 189, 95
- Peimbert M., 1967, *ApJ*, 150, 825
- Pilyugin L.S., 1992, *A&A*, 260, 58
- Pilyugin L.S., 1994, *AZh*, 71, 825
- Pilyugin L.S., 2000, *A&A*, 362, 325
- Pilyugin L.S., 2001a, *A&A*, 369, 594
- Pilyugin L.S., 2001b, *A&A*, 374, 412
- Pilyugin L.S., 2003a, *A&A*, 397, 109
- Pilyugin L.S., 2003b, *A&A*, 399, 1003
- Pilyugin L.S., 2005, *A&A*, 436, L1
- Pilyugin L.S., Edmunds M.G., 1996a, *A&A*, 313, 783
- Pilyugin L.S., Edmunds M.G., 1996a, *A&A*, 313, 792
- Pilyugin L.S., Ferrini F., 1998, *A&A*, 336, 103
- Pilyugin L.S., Thuan, T.X., Vílchez J.M., 2006a, *MNRAS*, 367, 1139
- Pilyugin L.S., Vílchez J.M., Contini T., 2004, *A&A*, 425, 849
- Pilyugin L.S., Vílchez J.M., Thuan, T.X., 2006b, *MNRAS*, 370, 1928
- Portinari L., Chiosi C., Bressan A., 1988, *A&A*, 334, 505
- Richer M.G., McCall M.L., 1995, *ApJ*, 445, 642
- Romano D., Chiappini C., Matteucci F., Tosi M., 2005, *A&A*, 430, 491
- Salpeter E.E., 1955, *ApJ*, 121, 161
- Schaller G., Schaerer D., Meynet G., Maeder A., 1992, *A&AS*, 96, 269
- Searle L., 1971, *ApJ*, 168, 327
- Simón-Díaz S., Herrero A., Esteban C., Najarro F., *A&A*, 448, 351
- Smith H.E., 1975, *ApJ*, 199, 591
- Stasińska G., 2005, *A&A*, 434, 507
- Timmes F.X., Woosley S.E., Weaver T.A., 1995, *ApJS*, 98, 617
- Tosi M., 1988a, *A&A*, 197, 33
- Tosi M., 1988b, *A&A*, 197, 47
- Tremonti C.A., et al., 2004, *ApJ*, 613, 898
- van den Hoek L.B., Groenewegen M.A.T., 1997, *A&AS*, 123, 305
- van Zee L., Salzer J.J., Haynes M.P., O'Donoghue A.A., Balonek T.J., 1998, *AJ*, 116, 2805
- Vila-Costas, M.B., Edmunds M.G., 1992, *MNRAS*, 259, 121
- Woosley S.E., Weaver T.A., 1995, *ApJS*, 101, 181
- Zaritsky D., Kennicutt R.C., Huchra J.P., 1994, *ApJ*, 420, 87